Resonances with natural and unnatural parities in positron-sodium scattering

Muhammad Umair* and Svante Jonsell†
Department of Physics, Stockholm University, SE-10691 Stockholm, Sweden
(Received 26 February 2015; revised manuscript received 23 April 2015; published 20 July 2015)

We present an investigation of resonances in positron-sodium scattering using the complex scaling method. For the target sodium atoms, the interaction between the core and outer electron is treated using two different types of analytical model potentials. Explicitly correlated Gaussian wave functions are used to represent the correlation effects between the outer electron, the positron, and the Na^+ core. S-, P-, and D-wave resonances with natural parity have been calculated for energies extending up to the positronium $n = 2$ formation threshold. Resonance states for unnatural parities P^e and D^0 have been calculated for energies extending up to the positronium $n = 3$ threshold. Below both positronium thresholds we have for each symmetry identified a dipole series of resonances, with binding energies scaling in good agreement with expectations from an analytical calculation. The presented results are compared with other theoretical calculations.

DOI: 10.1103/PhysRevA.92.012706 PACS number(s): 34.80.Uv, 36.10.Dr, 31.15.−p

I. INTRODUCTION

Over the past few years the study of atomic resonances with positrons has attracted a lot of interest in the field of positron-atom interactions [1–12]. The phenomena of resonances have been studied widely in positron-hydrogen scattering since Mittleman [13] suggested their existence.

Only a few theoretical studies have been made on resonances for the positron-sodium system. In a pioneering work Ward *et al.* [14] performed calculations of the positron-sodium system using the five-state close-coupling method. Recently, the stabilization method was applied to evaluate the resonances in this system by Kar and Ho [9] using Hylleraas functions and by Han *et al.* [10] using hyperspherical coordinates. Finally, Jiao *et al.* [15] studied higher partial-wave resonance states using the momentum-space coupled-channel optical method. While reasonable agreement has been reached between the two groups using the stabilization method, their calculations concentrate on only S-wave symmetry and relatively low energies. The groups using other methods include partial waves up to D waves and show fair agreement among one other but agree less well with the methods using the stabilization method.

There have been some experimental measurements of the total cross section [16,17] and of positronium (Ps) formation [18,19] for $e^{\pm}$-Na scattering, but not with sufficient energy resolution to map out the resonance structure.

Resonances with unnatural parity satisfy $\pi = (-1)^{J+1}$, where J is the total orbital angular momentum (the spin is conserved) of the system and π is the parity. Some work on unnatural-parity resonances for positron-hydrogen scattering has been performed [20–22], but positron-sodium scattering has not yet been examined. Recently, Bromley *et al.* performed a calculation of some unnatural parity bound states in positronic complexes [23].

In this study, we report resonances in the positron-sodium system determined using the complex scaling method for natural and unnatural parity. The e^+-Na system can be formulated as a three-body system: a frozen core, a positron, and an electron. In this way, the system resembles the hydrogen-positron system, but there are some qualitative differences. First, the interaction between the Na^+ core and the active electron is Coulombic only at very long range. At shorter distances the nuclear charge is only partially screened, which makes it necessary to employ some sort of model potential for the e^--Na^+ interaction. More generally this interaction should also include electron exchange, but this has not been explicitly included in our study. The e^+-Na interaction is, like the e^+-H interaction, at long distances dominated by the polarizability of the atom, giving a potential $\propto r^{-4}$. The polarizability of Na (162 a.u.) [24] is, however, larger than that of H (4.5 a.u.), which allows the formation of a truly bound state of the e^+-Na system [25]. Furthermore, the hydrogen atom has energy levels degenerate with respect to orbital angular momentum (neglecting fine structure), whereas the alkali atoms do not. Another characteristic of a positron-Na system is that the ionization energy of Na (0.19 a.u.) [26] is smaller than the binding energy of Ps (0.25 a.u.), allowing for positronium formation even at zero impact energy.

Our calculation is based on the coupled rearrangement channels method developed by Kamimura and coworkers [27,28]. Of the earlier works, our method is most similar to the stabilization method [9,10] but allows more accurate description of resonances by going into the complex plane. It is also different in the coordinate system and functional forms it uses for representing the wave function, allowing relatively large basis sets to be used. We have investigated two different types of analytical model potentials for the interaction between the core and the outermost active electron in our analysis.

Atomic units are used unless otherwise is specified.

II. METHOD

The Hamiltonian H of the system is given by

$$H = -\frac{1}{2\mu}\nabla_1^2 - \frac{1}{2\mu}\nabla_2^2 + V^{(e^-)}(r_1) + V^{(e^+)}(r_2) - \frac{1}{r_{12}}, \quad (1)$$

where the subscripts 1 and 2 denote the coordinates of the outer electron and positron, respectively; r_{12} is the relative distance between them. $V^{(e^-)}$ and $V^{(e^+)}$ are the interaction potentials

*muhammad.umair@fysik.su.se
†jonsell@fysik.su.se

TABLE I. Ground-state energy of the e^+-Na system calculated using different models. The results are compared to the result of Han *et al.* [10] using the same model potential as our MP2a, but with an additional term analogous to a "dielectronic correction" added to the e^+–e^- interaction to cancel the core polarization when the two particles coalesce. We have also included the result of Kubota and Kino [11], which uses the same numerical method but a different form of the model potential.

Model	Energy
MP1	−0.250312
MP2a	−0.250710
MP2b	−0.250337
Han *et al.* [10]	−0.250447
Kubota and Kino [11]	−0.250401

between the core of the sodium atom and the outer electron and the positron, respectively. For the electron interaction with the Na^+ core a model potential is required. In principle any model potential that accurately reproduces the atomic Na energy levels can be used. In order to assess the size of the uncertainty in the results coming from the form of the model potential we have tried and compared two different models used previously in [9] and [10]. These model potentials have the form of screened Coulomb interactions. For both model potentials the Coulomb part $\pm 1/r$ was treated analytically, while the remaining screening terms were fitted to a number of Gaussians. In this way we were able to represent the potential using a functional form which allows the Hamiltonian matrix elements to be calculated analytically, including when complex scaling is used.

Our first model (MP1) is the same as that used by Kar and Ho [9], given by

$$V^{(e^-)}(r) = -\frac{1}{r}[1 + (Z-1)\exp(-c_1 r) + c_2 r \exp(-c_3 r)], \tag{2}$$

where c_1, c_2, and c_3 are variational parameters; $Z = 11$ for Na. For e^+-Na scattering, we set $c_1 = 7.902$, $c_2 = 23.51$, and $c_3 = 2.688$, as suggested by Hanssen *et al.* [29] and Schweizer and Fabbinder [30]. For $V^{(e^+)}$ we use the same potential as in Eq. (2) but with an opposite sign. Using MP1 we have verified that the ground-state energy of the e^+-Na system (see Table I) and also the ground- and excited-state energies of Na (shown in Table II) agree with other calculations and with experimental values [26]. Thus, we conclude that our fit to Gaussians is accurate enough to obtain good energies. For the e^+-Na interaction we also tried an effective potential calculated using the Hartree-Fock (HF) method, as was suggested in [9]. The difference in the results turned out to be marginal, as can be expected because of the repulsive interaction that does not allow the positron to penetrate the core. The corresponding modification to the attractive e^--Na^+ interaction should probably give a larger change. In this case, however, the HF potential cannot be used because, first, it does not include exchange with the valence electron and, second, it does not reproduce the correct atomic thresholds of the Na atom with sufficient accuracy.

TABLE II. Comparison of calculated binding energies of the Na atom using different model potentials for the core–valence-electron interaction. The excited-state energies are calculated relative to the ground state of the Na atom. The experimental energies are calculated using the ionization energy 0.188857595 a.u. [26] and the weighted averages of the excitation energies of all fine-structure levels [26].

	Present results		
State	MP1	MP2	Experiment [26]
$3s$	0.18886	0.18886	0.18886
$3p$	0.11152	0.11154	0.11154
$4s$	0.07167	0.07158	0.07158
$3d$	0.05598	0.05595	0.05594
$4p$	0.05102	0.05094	0.05093
$5s$	0.03763	0.03758	0.03758
$4d$	0.03150	0.03143	0.03144
$4f$	0.03134	0.03126	0.03127
$5p$	0.02924	0.02917	0.02919

The second model potential (MP2) used for the valence-electron–core interaction is the same as that used by Han *et al.* [10] and has the form

$$V_-(r) = -\frac{1}{r}[Z_c + (Z - Z_c)e^{-a_1 r} + a_2 r e^{-a_3 r}] - \frac{a_c}{2r^4}\left[W_3\left(\frac{r}{r_c}\right)\right]^2, \tag{3}$$

where

$$W_3(r) = 1 - e^{-r^3} \tag{4}$$

is the cutoff function employed to determine the correct behavior at the origin. The second term in Eq. (3) arises from the polarization of the core, where $a_c = 0.9457$ is the Na^+ polarizability [31]. The $1/r^4$ tail of the potential cannot be fitted well using Gaussians. Therefore, in order to get this long-range part of the potential correctly, the term

$$U_{\rm pol}(r) = -\frac{a_c}{2r^4}(1 - e^{-r^2})^2, \tag{5}$$

which can be calculated analytically (i.e., without fitting to Gaussians), was treated separately, while the remainder $V_-(r) - U_{\rm pol}(r)$ was fitted to Gaussians using the same procedure as described above, i.e., treating the Coulomb part analytically while fitting the remaining screening function. [Note that this form differs from (4) but also has the property that it does not diverge at $r = 0$, although it differs in that it does not vanish in this limit. The term in (5) gives a matrix element which is much easier to calculate analytically when Gaussian basis functions are used.]

Also in Eq. (3), the nuclear charge is $Z = 11$, and the charge of the Na^+ core is $Z_c = 1$. The other parameters were fitted by Liu and Starace [32] to reproduce the experimentally measured energy levels of the Na atom. Their values are $a_1 = 3.32442452$, $a_2 = 0.71372798$, $a_3 = 1.83281815$, and $r_c = 0.52450638$. The atomic Na energies calculated with our implementation of this model are also shown in Table II, again confirming that our fit is accurate.

For $V^{(e^+)}$ we used the same potential as in Eq. (3) but with a reversed sign of the first term, while the second term represents that the (always attractive) polarizability was first left unchanged (MP2a). However, this leads to a double counting of the core polarization when the electron and positron coalesce, while physically there should be no polarization induced by the interaction with a neutral system. In [10] this problem was solved by introducing an additional term in the electron-positron interaction, but the form of this term, containing a product of coordinates belonging to different rearrangement channels, would be very difficult to use in our method. Instead, we have tried to determine the error introduced by this imperfection by also comparing it to calculations where we also reversed the sign of the polarization term (MP2b). We found that changing this sign does have a significant impact on the ground state of the e^+-Na system (see Table I). However, we also found that for resonances the difference between MP2a and MP2b is much smaller, only about 10^{-6} a.u. Results for resonances using MP1 and MP2a are compared in Tables III and VII.

The correlation effects between the electron, the positron, and the core were calculated using the coupled rearrangement channels method developed by Kamimura and coworkers [27,28]. In this method the wave function is expanded using Jacobi coordinates $(\{\mathbf{r}_i, \mathbf{R}_i\}, i = 1,2,3)$ in all three possible rearrangement channels. This gives a very versatile basis set, capable of adapting to states close to the breakup thresholds of any pair of particles.

Within this coordinate system we represent the wave function using a partial-wave expansion of the angular variables and Gaussians in the radial variables. That is, for a state with total orbital angular momentum J, M the wave function has the form

$$\Psi_{JM} = \sum_{\alpha=1}^{3} \sum_{l_\alpha=0}^{l_\alpha^{\max}} \sum_{L_\alpha=0}^{L_\alpha^{\max}} \sum_{i=1}^{i_{\alpha l}^{\max}} \sum_{I=1}^{I_{\alpha L}^{\max}} c_{\alpha l_\alpha L_\alpha i I} \phi_{\alpha l_\alpha L_\alpha i I}, \tag{6}$$

$$\phi_{\alpha l_\alpha L_\alpha i I} = N_{\alpha l_\alpha L_\alpha i I} r_\alpha^{l_\alpha} R_\alpha^{L_\alpha} e^{-(r_\alpha/r_{\alpha l_\alpha i})^2} e^{-(R_\alpha/R_{\alpha L_\alpha I})^2} \times [Y_{l_\alpha}(\hat{\mathbf{r}}_\alpha) \otimes Y_{L_\alpha}(\hat{\mathbf{R}}_\alpha)]_{JM}. \tag{7}$$

Here α denotes the three rearrangement channels, l_α and L_α are the angular momenta along $\mathbf{r}_\alpha$ and $\mathbf{R}_\alpha$, respectively, and i and I are numbers of Gaussians along the two radial coordinates. The angular momenta l_α and L_α are chosen to be consistent with the total J (i.e., $|l_\alpha - L_\alpha| \leqslant J \leqslant l_\alpha + L_\alpha$, up to some maximum values $l_\alpha^{\max}$ and $L_\alpha^{\max}$, which may be different for different rearrangement channels.) The total numbers of Gaussian trial functions for each rearrangement channel and angular momentum are given by $i_{\alpha l}^{\max}$ and $I_{\alpha L}^{\max}$. $N_{\alpha l_\alpha L_\alpha i I}$ is a normalization constant ensuring that $\langle \phi_{\alpha l_\alpha L_\alpha i I} | \phi_{\alpha l_\alpha L_\alpha i I} \rangle = 1$. The widths of the Gaussians $r_{\alpha l_\alpha i}$ and $R_{\alpha L_\alpha I}$ are, for each channel and set of angular momenta, chosen as geometric progressions,

$$r_{\alpha l_\alpha i} = r_{\alpha l_\alpha 1} \left(\frac{r_{\alpha l_\alpha i_{\alpha l}^{\max}}}{r_{\alpha l_\alpha 1}} \right)^{\frac{i-1}{i_{\alpha l}^{\max}-1}},$$

$$R_{\alpha L_\alpha I} = R_{\alpha L_\alpha 1} \left(\frac{R_{\alpha L_\alpha I_{\alpha L}^{\max}}}{R_{\alpha L_\alpha 1}} \right)^{\frac{I-1}{I_{\alpha L}^{\max}-1}}, \tag{8}$$

where the smallest and largest values $\{r_{\alpha l_\alpha 1}, r_{\alpha l_\alpha i_{\alpha l}^{\max}}, R_{\alpha L_\alpha 1}, R_{\alpha L_\alpha I_{\alpha L}^{\max}}\}$ are set explicitly and used as nonlinear variational parameters. In this way most Gaussians will span the short to medium range, while a few more diffuse Gaussians capture the long-range part of the wave function. In this work, resonances with very small binding energies have been calculated, and hence, it was essential to set a large enough value for the outer radius R_i.

Resonances are calculated using the complex scaling method (also known as the complex coordinate rotation method) [2,33–35]. The complex dilation operator $U(\theta)$ acting on a function $f(\mathbf{r})$ is defined through

$$U(\theta) f(\mathbf{r}) = e^{3i\theta/2} f(e^{i\theta}\mathbf{r}), \tag{9}$$

where the exponential prefactor ensures that the complex scaled function satisfies the normalization condition $\int U(\theta) f^*(\mathbf{r}) U(\theta) f(\mathbf{r}) \mathrm{d}^3 r = 1$. The corresponding transformation of the Hamiltonian is, for the special case $V \propto 1/r$,

$$H(\theta) = U(\theta) H U^{-1}(\theta) = e^{-2i\theta} T + e^{-i\theta} V, \tag{10}$$

and, more generally, $U(\theta) V(r) U^{-1}(\theta) = V(e^{i\theta} r)$. For simple functional forms, such as Gaussians and polynomials, it is easy to implement the complex scaling. Stationary eigenvalues of the complex scaled generalized eigenvalue problem

$$\tilde{H}(\theta) c^\theta = E \tilde{S} c^\theta, \quad \tilde{H}_{ij}(\theta) = \langle \psi_i | H(\theta) | \psi_j \rangle,$$
$$\tilde{S}_{ij}(\theta) = \langle \psi_i | \psi_j \rangle \tag{11}$$

TABLE III. Comparison of our results for S-, P-, and D-wave resonance energies E_R and widths Γ in the e^+-Na system. The threshold energies shown here are calculated using the respective model potential (see Table II) and are close to the experimental values. The notation $x[y]$ means 10^{-y}.

	MP1		MP2a	
Resonance	E_R	Γ	E_R	Γ
S	−0.076839	1.54[4]	−0.076789	1.51[4]
P	−0.075238	1.09[4]	−0.075195	1.00[4]
D	−0.072653	2.68[4]	−0.072596	4.96[4]
Na(4s)	$E_t = -0.07167$		$E_t = -0.07158$	
S	−0.066615	7.20[5]	−0.066596	6.91[5]
	−0.063628	1.62[5]	−0.063622	1.61[5]
	−0.062803	4.16[6]	−0.062802	4.34[6]
	−0.062581	1.14[6]	−0.062581	1.16[6]
	−0.062522	3.10[7]	−0.062522	3.07[7]
	−0.062506	8.68[8]	−0.062506	8.21[8]
P	−0.065813	5.28[5]	−0.065800	4.77[5]
	−0.063364	5.76[5]	−0.063364	5.51[5]
	−0.063071	1.90[4]	−0.063063	1.99[4]
	−0.062704	3.70[6]	−0.062703	4.50[6]
	−0.062552	8.12[7]	−0.062551	8.17[7]
	−0.062513	1.89[7]	−0.062513	1.11[7]
D	−0.064657	1.53[4]	−0.064644	1.70[4]
	−0.062957	3.50[5]	−0.062950	2.57[5]
	−0.062599	8.16[6]	−0.062595	5.58[6]
	−0.062522	1.83[6]	−0.062520	1.35[6]
Ps($n = 2$)	$E_t = -0.062500$			

TABLE IV. Comparison of the S-, P-, and D-wave resonance energy E_R and width Γ for the e^+-Na system with other calculations, calculated using model potential MP2a. The threshold energies are calculated using the same model potential (right column of Table II). The notation $x[y]$ means 10^{-y}.

	Present results (MP2a)		Ward *et al.* [14]		Kar and Ho [9]		Han *et al.* [10]		Jiao *et al.* [15]	
Resonance	E_R	Γ	E_R	Γ	E_R	Γ	E_R	Γ	E_R	Γ
S	−0.076789	1.51[4]	−0.07144	7.3[6]	−0.07582	4.3[4]	−0.0768010	1.4[4]	−0.08155	5.55[4]
P	−0.075195	1.00[4]	−0.07405	1.2[3]					−0.07787	3.36[3]
D	−0.072596	4.96[4]	−0.071	1.1[3]					−0.07313	6.44[3]
				Na(4s) threshold ($E_t = -0.07158$)						
S	−0.066596	6.10[5]			−0.06591	3.1[4]	−0.0665606	6.1[5]	−0.06641	2.01[3]
	−0.063622	1.61[5]					−0.0635301	4.1[5]		
				Ps($n = 2$) threshold ($E_t = -0.06250$)						

correspond to complex energies $E = E_R - i\Gamma/2$ of the system, where E_R is the resonance energy and Γ is the width.

III. RESULTS AND DISCUSSION

A. e^+-Na resonances with natural parity

Resonance positions and widths found in the e^+-Na system with natural parity are summarized for S-, P-, and D waves in Tables III and IV. Our results were obtained using about 7000 Gaussian basis functions with different possible combinations for angular momentum, with maximum values $l_\alpha^{\max} = L_\alpha^{\max} = 4$. In Table III, we compare our results using the two different model potentials, whereas in Table IV we compare our results to the results obtained in other studies (when available). In Table IV we give our results using MP2a (see above). We find that the uncertainty arising from using different model potentials is much smaller than the differences between earlier calculations reported in the literature. We estimate that the numerical uncertainties for the resonance energies and widths are within a few parts of the last quoted digit.

Earlier works have also reported a number of near-threshold resonances for which we have not found evidence [9,10,14,15]. The parameters for these resonances, as reported in other papers, are summarized in Table V. All previous works have found resonances close to the $3p$ threshold of S-wave and P-wave symmetry (only two calculations included P waves). A closer look at the resonance parameters reveals fair agreement between the work by Ward *et al.* using the close-coupling method [14] and that by Jiao *et al.* using the coupled-channels optical method [15]. The main difference between these two works is that Jiao *et al.* [15] included Ps channels, which were not included at all by Ward *et al.* [14]. The two calculations by Kar and Ho [9] and by Han *et al.* [10], both using the stabilization method, on the other hand, differ quite a lot from these and also between each other. In fact, according to these works the resonance lies on the other side of the Na($3p$) threshold, i.e., just above it. It was speculated in [10] that these could be shape resonances supported by the adiabatic correction to the hyperspherical potential curves, which creates a small barrier and thus slightly increases the effective depth of the potential. We find this explanation unlikely as the barrier does not seem to be high enough to support the resonance. Close to the $4s$ threshold another S-wave resonance has been reported by Han *et al.* [10]. The other works have not found this resonance.

We note that when using the stabilization technique, it can be difficult to discriminate between resonances and low-energy continuum states since the energies of both vary very little as the scale of the system is changed. Indeed, we have also performed stabilization (real scaling) calculations, where we found states looking similar to resonances just above the Na($3p$) threshold [Fig. 1(a)]. Zooming in on the state does, however, reveal a small variation with the scaling parameter α [Fig. 1(b)], and the continuum-state nature of the state is confirmed by the complex scaling method [Fig. 1(c)]. We have made considerable efforts to search for resonances in this energy region by trying many different basis sets but have not found any. In contrast, a typical complex scaling graph for a resonance is shown in Fig. 2.

Between the Na($3p$) and Na($4s$) thresholds we found one resonance for each angular momentum $J = 0$, 1, and

TABLE V. Resonance parameters for near-threshold resonances as reported in earlier publications. These resonances were not found by us. The energy ϵ is the energy relative to the atomic threshold in the leftmost column (calculated using the numerical results for the atomic threshold as obtained in the respective publications). The notation $x[y]$ means 10^{-y}.

		Ward *et al.* [14]			Kar and Ho [9]			Han *et al.* [10]			Jiao *et al.* [15]		
Threshold	J	E_R	ϵ	Γ	E_R	ϵ	Γ	E_R	ϵ	Γ	E_R	ϵ	Γ
$3p$	0	−0.1159	−4.3[3]	1.5[5]	−0.10732	4.20[3]	2.0[4]	−0.1108330	7.05[4]	4.1[5]	−0.1164	−4.8[3]	1.31[3]
$3p$	1	−0.1130	−1.4[3]	2.2[4]							−0.1131	−1.6[3]	1.75[3]
$4s$	0							−0.0709401	6.40[4]	4.7[5]			

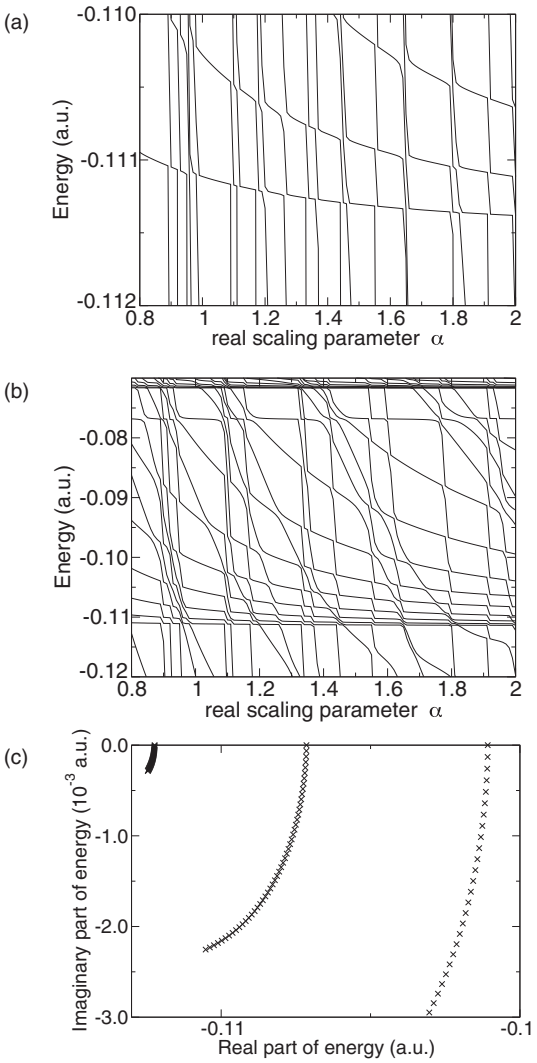

FIG. 1. (a) and (b) Real and (c) complex stabilization graphs of e^+-Na states around the Na($3p$) threshold. The $3p$ threshold opens at -0.1115 a.u. All states which curve down as α is increased are continuum states, with the curvature depending on which threshold they belong to. The flat plateau at -0.0768 a.u. is a resonance. The $4s$ threshold opens at -0.0716 a.u. The flat plateau just above the $3p$ threshold is not a resonance, as is revealed by zooming in on the state (b) or going into the complex plane (c).

2. We have not made any calculations for higher angular momenta. The uncertainty introduced from different model potentials is less than 10^{-4} a.u. The S-wave resonance energy of -0.076789 a.u. and width of 1.51×10^{-4} a.u. agree very well with the results by Han *et al.* [10] but are quite a bit higher in energy than the result by Jiao *et al.* [15].

For P and D waves, we have different possible combinations of the individual angular momenta (l_α, L_α). The total number of configurations used was 24. Our results in Table IV are compared with those of Ward *et al.* and Jiao *et al.* [14,15]. The energies are in fair agreement with the other available results, but the widths we obtained are considerably smaller.

Most of the resonances located above the Na($4s$) threshold belong to the dipole series converging to the Ps($n = 2$) threshold, which is discussed in Sec. III C.

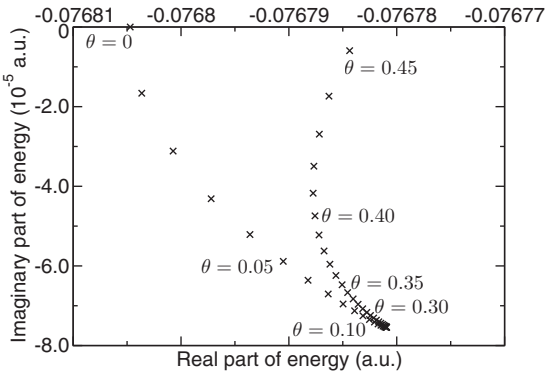

FIG. 2. Complex scaling graph for a resonance. The crosses show the energy eigenvalues in the complex plane as a function of the complex scaling parameter θ in steps of 0.01. The stationary point, indicating the presence of a resonance, is plainly visible. Note that the real part of the energy E_R is shifted up by 2.4×10^{-5} a.u. compared to the result using the real stabilization method ($\theta = 0$).

B. e^+-Na resonances with unnatural parity

We have also calculated resonance states with so-called unnatural parity, i.e., parity $-(-1)^J$. Since the parity of the state is given by $(-1)^{l_\alpha + L_\alpha}$, unnatural-parity states are obtained by choosing basis functions with angular momentum such that $(-1)^{l_\alpha + L_\alpha + J} = -1$. Adding the requirement that $|l_\alpha - L_\alpha| \leqslant J \leqslant l_\alpha + L_\alpha$ makes it plain that unnatural-parity resonances exist for $J \geqslant 1$. Table VI shows the total number of basis functions used for a given angular momentum state, as well as the individual (l_α, L_α) pairs for different angular momentum combinations. N is the number of configurations used.

For the P^e states, both the electron and positron have the same angular momentum, which couple to form the total orbital angular momentum $J = 1$ shown in Table VI. The numerical results are shown in Table VII. The lowest unnatural-parity resonance state is located at the energy position $E_R = -0.062923$ a.u. with a width $\Gamma = 6.00 \times 10^{-6}$ a.u. lying below the Ps($n = 2$) threshold. The next two P^e resonances lie below the $4d$ threshold. Similar to the case for natural parity, the resonances lying below the Ps($n = 3$) threshold are members of a dipole series. For the D^0 symmetry, we found ten resonances, shown in Table VII.

C. Dipole series

In contrast to hydrogen, the energy levels of Na are not degenerate with respect to the L quantum number. Thus, there is no linear Stark effect in Na; that is, the interaction with the positron cannot, to first order, induce a dipole moment (but to second order the polarizability gives a long-range potential $\sim r^{-4}$ as discussed above). However, the energy levels of Ps

TABLE VI. States with total orbital angular momentum J and parity $\pi = (-1)^{J+1}$.

State	J	(l_α, L_α)	N	Total basis
P^e	1	(1,1),(2,2),(3,3),(4,4)	12	7200
D^0	2	(2,1); (1,2),(3,2); (2,3),(4,3); (3,4)	18	8200

TABLE VII. Unnatural-parity resonance energy E_R and width Γ for P^e and D^0 waves in the e^+-Na system. The notation $x[y]$ means 10^{-y}.

	MP1		MP2a	
Resonance	E_R	Γ	E_R	Γ
P^e	−0.062924	6.24[6]	−0.062923	6.00[6]
Ps($n=2$)		($E_t=-0.062500$)		
P^e	−0.035141	5.00[5]	−0.035120	5.24[5]
	−0.031872	2.26[5]	−0.031841	2.30[5]
D^0	−0.034500	4.13[5]	−0.034479	4.15[5]
	−0.031736	5.79[6]	−0.031708	5.75[6]
	−0.031594	3.47[5]	−0.031571	3.54[5]
Na($4d$)	($E_t=-0.03150$)		($E_t=-0.03143$)	
D^0	−0.031404	1.36[4]	−0.031328	1.10[4]
Na($4f$)	($E_t=-0.03134$)		($E_t=-0.03126$)	
P^e	−0.029897	3.88[4]	−0.029898	3.59[4]
D^0	−0.029530	1.97[4]	−0.029524	1.97[4]
Na($5p$)	($E_t=-0.02924$)		($E_t=-0.02917$)	
P^e	−0.028454	1.06[4]	−0.028453	1.25[4]
	−0.027994	3.88[5]	−0.027994	3.94[5]
	−0.027848	1.25[5]	−0.027848	1.27[5]
	−0.027801	4.08[6]	−0.027801	4.14[6]
	−0.027785	1.33[6]	−0.027785	1.36[6]
D^0	−0.028287	8.63[5]	−0.028285	8.76[5]
	−0.027924	2.86[5]	−0.027924	2.84[5]
	−0.027821	7.87[6]	−0.027821	7.94[6]
	−0.027791	2.34[6]	−0.027791	2.36[6]
	−0.027782	3.22[7]	−0.027781	2.92[7]
Ps($n=3$)		($E_t=-0.027778$)		

are degenerate with respect to the l quantum number, and hence, the Ps-Na^+ interaction does to first order give a dipole interaction, i.e., an interaction-potential with long-range form proportional to $-1/r^2$. This long-range potential gives, in principle, an infinite sequence of quasibound states clustering towards the Ps thresholds, starting at the $n=2$ threshold. The binding energies (and widths) of each sequence follow a fixed ratio,

$$\frac{\epsilon_n}{\epsilon_{n+1}} = \exp\left(\frac{2\pi}{\alpha}\right), \tag{12}$$

where the parameter α is unique to each Ps threshold, total orbital angular momentum J, and parity of the system but universal with respect to any positive ion it interacts with. A universal formula for α, calculated using the methods of Temkin and Walker [36], is given in the Appendix. The results are summarized in Table VIII, where they are also compared to the results for hydrogen. Note that the different mass factors in Ps compared to those in H results in a much closer energy spacing between the dipole states in Ps. Hence, it is possible to find a larger number of dipole states below Ps thresholds. The range of binding energies over which the scaling is valid is limited from above by $\epsilon \ll 1/n^4$ and at the limit of small binding energies by the size of the fine structure in Ps (which is of the order of 10^{-6}).

TABLE VIII. Dipole series for Ps and H, the parameter α (see text), and energy ratios. For some symmetries more than one solution exists.

			Ps		H	
n	J	Parity	α	$\epsilon_n/\epsilon_{n+1}$	α	$\epsilon_n/\epsilon_{n+1}$
2	0	+	4.77	3.73	2.20	17.43
2	1	−	4.58	3.95	1.86	29.33
2	2	+	4.16	4.54	0.75	4422
3	0	+	7.74	2.25	3.64	5.61
3	1	+	5.64	3.05	2.23	16.75
3	1	−	7.94	2.21	3.74	5.35
3	1	−	4.70	3.80	1.82	31.32
3	2	+	6.88	2.49	3.07	7.73
3	2	+	3.48	6.07		
3	2	−	5.30	3.28	1.43	80.55

The resonances closest to threshold are extremely narrow and need very high accuracy for the calculation. Our numerical results for the scaling of the dipole states are given in Tables IX and X. At the $n=2$ threshold (Table IX) we find that the scaling of the S-wave binding energies is in excellent agreement with the expected scaling. For P and D states the agreement is slightly less good but still fair. The P-wave resonance located at $E_R=-0.063063$ a.u. does not seem to fit into the dipole sequence and has been omitted in Table IX. The differences probably arise from numerical inaccuracies in the calculation of these very extended and weakly bound states. The widths are less accurate, although still reasonable, except for the resonances of P symmetry. It is possible that these resonances are distorted by the proximity to the nondipole resonance at $E_R=-0.063063$ a.u. It is not surprising that the widths are less accurate since, in general, it is more difficult to obtain accurate widths, especially when they are very small (of the order of 10^{-5} a.u. or less), as in this case. We also see that the scaling of the first few resonances in the series diverges slightly more from the analytical result. This is likely to be physical, as the conditions for the validity of the analytical representation are not fully satisfied when the binding energy is too large. Referring to Table III, we also see that the position of the resonances changes very little with the different model potentials. Thus, as could be expected, the polarization of the Na^+ core does not play a vital role in the formation of the resonances in the Ps dipole series.

Turning to the unnatural-parity case there is no dipole series at the $n=2$ threshold. The reason is that the dipole moment at $n=2$ can only come from the coupling of the degenerate $2s$ and $2p$ states in Ps. However, in the coupling scheme leading to unnatural parity, S waves are not permitted (see Table VI). Instead, the first dipole series arises below $n=3$, with the dipole coming from the coupling of the degenerate $3p$ and $3d$ Ps states.

At the $n=3$ threshold we have extracted only resonance parameters for the unnatural-parity case because for the normal parity the number of states gets very large, which makes it hard to identify the resonances. The agreement is still fair, at least for the P^e symmetry. For the D^0 symmetry the error is of the

TABLE IX. Energy and width ratios of successive resonances located by the present calculation for Ps($n = 2$).

$\mathcal{E}_j/\mathcal{E}_{j+1}$	Numerical result	Analytical value
	S wave	
1/2	3.65	3.73
2/3	3.72	
3/4	3.73	
4/5	3.73	
5/6	3.73	
	P wave	
1/2	3.82	3.95
2/3	4.26	
3/4	3.95	
4/5	4.04	
	D wave	
1/2	4.76	4.54
2/3	4.73	
3/4	4.67	
Γ_j/Γ_{j+1}	Numerical result	Analytical value
	S wave	
1/2	4.29	3.73
2/3	3.71	
3/4	3.74	
4/5	3.78	
5/6	3.73	
	P wave	
1/2	0.87	3.95
2/3	12.23	
3/4	5.52	
4/5	7.35	
	D wave	
1/2	6.64	4.54
2/3	4.59	
3/4	4.12	

same order as the difference between the results using different model potentials. The results are shown in Table X.

IV. CONCLUSION

In conclusion, we have investigated resonance phenomena in e^+-Na scattering. Resonance states with total orbital angular momentum $J = 0$–2 have been obtained for natural parity. Resonance positions and widths have been compared with other theoretical results. We have compared model potentials for the e^--Na^+ and e^+-Na^+ interactions with and without a polarization term and found that the change in the resonance parameters is quite small, while the ground-state energy changes much more. The change in the results using different model potentials is not large enough to explain the difference between results obtained in earlier calculations [9,10,14,15]. Some resonances found in previous works could not be confirmed by our calculation. For other resonances fair agreement with earlier works was obtained, in particular with the calculation by Han *et al.* [10].

We have also reported resonances with unnatural parities. For both parities we find dipole series converging to Ps thresholds. The energy and width ratios of the successive resonances of these sequences were compared to analytical results. We found that the sequence binding energies of the S-wave resonances under Ps($n = 2$) converged to exactly the analytical results. For binding energies with higher L values the agreement was also fair, while for the widths the results were less accurate. This is probably due to numerical inaccuracies because of the difficulty in obtaining an extremely high numerical accuracy for a calculation adjacent to the threshold, where the states are very extended and widths are very small.

TABLE X. Energy and width ratios of successive resonances below the Ps($n = 3$) threshold with unnatural parity.

$\mathcal{E}_j/\mathcal{E}_{j+1}$	Numerical result	Analytical value
	P^e wave	
1/2	3.12	3.05
2/3	3.08	
3/4	3.06	
4/5	3.05	
	D^0 wave	
1/2	3.48	3.26
2/3	3.38	
3/4	3.31	
4/5	4.05	
Γ_j/Γ_{j+1}	Numerical result	Analytical value
	P^e wave	
1/2	3.17	3.05
2/3	3.10	
3/4	3.07	
4/5	3.06	
	D^0 wave	
1/2	3.08	3.26
2/3	3.58	
3/4	3.36	
3/5	8.08	

At the present time there are no experimental results with energy resolution high enough to map out the resonance structure. However, in recent years there has been rapid progress in the development of positron beams with high-energy resolution [37], and we hope that in the future such studies will become available.

ACKNOWLEDGMENT

This work was supported by the Swedish Research Council (VR).

APPENDIX: DIPOLE INTERACTION

The dipole series can be analyzed using a treatment very similar to the one used for H^- by Temkin and Walker [36]. The long-range form of the wave function under the Ps threshold n can be expressed as

$$\Psi(\boldsymbol{r},\boldsymbol{\rho}) \to \sum_{l,L} v_{Ll}(\rho) R_{nl}(r) [Y_l(\hat{\boldsymbol{r}}) \otimes Y_L(\hat{\boldsymbol{\rho}})]_{JM_J}, \qquad \text{(A1)}$$

where $\boldsymbol{r}$ and $\boldsymbol{\rho}$ are the internal and the center-of-mass coordinates of positronium, R_{nl} is the radial part of the Ps wave function, JM_J is the total orbital angular momentum, L is the orbital angular momentum of the Ps COM motion, and

$$[Y_l(\hat{\boldsymbol{r}}) \otimes Y_L(\hat{\boldsymbol{\rho}})]_{JM_J} = \sum_{m,M} \langle l\,L\,m\,M | J\,M_J\rangle Y_{lm}(\hat{\boldsymbol{r}}) Y_{LM}(\hat{\boldsymbol{\rho}}), \tag{A2}$$

with $\langle l\,L\,m\,M | J\,M_J\rangle$ being the Clebsch-Gordan coefficient. The sum in Eq. (A1) is restricted to terms for which $(-1)^{l+L+J} = 1$ (-1) for natural (unnatural) parity states. In the $\rho \to \infty$ limit the Hamiltonian is

$$\begin{aligned} \hat{H} &= \hat{H}_{\rm Ps} - \frac{1}{2M_{\rm Ps}}\Delta_{\boldsymbol{\rho}} + \frac{1}{|\boldsymbol{\rho} - \boldsymbol{r}/2|} - \frac{1}{|\boldsymbol{\rho} + \boldsymbol{r}/2|} \\ &\to \hat{H}_{\rm Ps} - \frac{1}{2M_{\rm Ps}}\Delta_{\boldsymbol{\rho}} + \frac{4\pi}{3}\frac{r}{\rho^2}\sum_{\nu=-1}^{1} Y_{1\nu}(\hat{\boldsymbol{r}}) Y^*_{1\nu}(\hat{\boldsymbol{\rho}}), \end{aligned}$$

with $\hat{H}_{\rm Ps}$ being the Hamiltonian for Ps and $M_{\rm Ps} = 2m_e$ being the Ps mass. In the limit of large ρ the Schrödinger equation reads

$$\left(-\frac{1}{2M_{\rm Ps}}\Delta_{\boldsymbol{\rho}} + \frac{4\pi}{3}\frac{r}{\rho^2}\sum_{\nu=-1}^{1} Y_{1\nu}(\hat{\boldsymbol{r}}) Y^*_{1\nu}(\hat{\boldsymbol{\rho}}) + \mathcal{E}_n - E\right) \times \Psi(\boldsymbol{r},\boldsymbol{\rho}) = 0, \tag{A3}$$

where $\mathcal{E}_n$ is the energy of the Ps states with principal quantum number n. Projection with the Ps(nlm) states gives a set of coupled equations,

$$\begin{aligned} &\left(-\frac{1}{2M_{\rm Ps}}\Delta_{\boldsymbol{\rho}} + \mathcal{E}_n - E\right) v_{L,l}(\rho) Y_{LM}(\hat{\boldsymbol{\rho}}) \\ &\quad - \frac{1}{\rho^2}\sum_{L'}\sum_{l'=0}^{n-1} v_{L'l'}(\rho)(-1)^{J+l+L} D^n_{ll'}\sqrt{(2l'+1)(2L'+1)} \\ &\quad \times \langle 1l'00|l0\rangle\langle 1L'00|L0\rangle \begin{Bmatrix} 1 & l' & l \\ J & L & L' \end{Bmatrix} Y_{LM}(\hat{\boldsymbol{\rho}}) = 0, \end{aligned} \tag{A4}$$

where l is chosen such that $|l - L| \leqslant J \leqslant l + L$, $l \leqslant n - 1$ and $(-1)^{l+L}$ gives the desired parity of the state. Here $D^n_{ll'} = \langle R_{nl}|r|R_{nl'}\rangle$ is the radial dipole element of the Ps state, and $\{\cdots\}$ is the Wigner $6j$ symbol. Note that because of the reduced mass difference, the dipole element for Ps is twice as large as that for the hydrogen atom.

The coupled equations (A4) can be expressed in terms of a nondiagonal potential matrix $\tilde{V}$ as

$$\left(\frac{\partial^2}{\partial\rho^2} - 2M_{\rm Ps}(\mathcal{E}_n - E + \tilde{V})\right)\tilde{f}(\rho) = 0, \tag{A5}$$

where $\tilde{f}(\rho)$ is the vector given by $f_i(\rho) = \rho v_{Ll}(\rho)$. On the diagonal the elements of $\tilde{V}$ are given by $-L(L+1)/(2M_{\rm Ps})$. The off-diagonal elements of the potential $\tilde{V}$ are proportional to the dipole matrix and further multiplied by $M_{\rm Ps}$, making the term overall 4 times larger than in the case of hydrogen. Diagonalizing $2M_{\rm Ps}\tilde{V}$ will give one negative root λ, which can support quasibound state through the long-range potential $-\lambda/\rho^2$. One finds that the corresponding long-range solution has the form $f(\rho) = \sqrt{\rho}H^{(1)}_{i\alpha}(i\sqrt{\epsilon}\rho)$, where $H^{(1)}_{i\alpha}$ is the first Hankel function, $\epsilon = 2M_{\rm Ps}(\mathcal{E}_n - E)$, and

$$\alpha = \sqrt{-1/4 - \lambda}. \tag{A6}$$

This solution is valid for $\rho \geqslant a$, where a is sufficiently large. The eigenvalues are determined by the short-range boundary condition at $\rho = a$. This boundary condition can be expressed as [36]

$$\frac{\alpha}{a}\cot[\alpha\ln(\sqrt{\epsilon}a/2) - \varphi] + \frac{1}{2a} = K, \tag{A7}$$

where $\varphi = \arg[\Gamma(1 + i\alpha)]$. Solving for ϵ gives,

$$\epsilon = \frac{4}{a^2}\exp\left\{\frac{2}{\alpha}\left[\cot^{-1}\left(K - \frac{1}{2a}\right)\frac{a}{\alpha} + n\pi + \varphi\right]\right\}. \tag{A8}$$

The term $n\pi$ (where n is an integer) comes from the periodicity of the cot function. Thus, the energies of consecutive solutions scale as

$$\frac{\epsilon_n}{\epsilon_{n+1}} = \exp\left(\frac{2\pi}{\alpha}\right), \tag{A9}$$

where α can be calculated analytically through (A6) and the diagonalization of the potential $\tilde{V}$ given by (A4).

The requirement for the validity of these solutions is that the boundary condition (A7) is valid (i.e., K does not depend on ϵ). This is true if $\epsilon \ll \lambda/a^2$. On the other hand, the long-range form of the potential is valid only for $a \gg r_0$, where $r_0 \sim n^2/\mu$ is set by the size of the Ps state, and $\lambda \sim M_{\rm Ps}/\mu$ from the diagonal elements of the long-range potential. That is, $\epsilon \ll M_{\rm Ps}\mu/n^4$.

[1] A. K. Bhatia and R. J. Drachman, Phys. Rev. A **42**, 5117 (1990).
[2] Y. K. Ho, Phys. Rep. **99**, 1 (1983).
[3] Y. K. Ho, Hyperfine Interact. **73**, 109 (1992).
[4] Y. K. Ho, Phys. Rev. A **53**, 3165 (1996).
[5] A. Igarashi and I. Shimamura, Phys. Rev. A **56**, 4733 (1997).
[6] K. Aiba, A. Igarashi, and I. Shimamura, J. Phys. B **40**, F9 (2007).
[7] Z.-C. Yan and Y. K. Ho, J. Phys. B **36**, 4417 (2003).
[8] A. Igarashi and I. Shimamura, Phys. Rev. A **70**, 012706 (2004).
[9] S. Kar and Y. K. Ho, Eur. Phys. J. D **35**, 453 (2005).
[10] H. Han, Z. Zhong, X. Zhang, and T. Shi, Phys. Rev. A **77**, 012721 (2008).
[11] Y. Kubota and Y. Kino, New J. Phys. **10**, 023038 (2008).
[12] U. Roy and Y. K. Ho, J. Phys. B **35**, 2149 (2002).
[13] M. H. Mittleman, Phys. Rev. **152**, 76 (1966).
[14] S. J. Ward, M. Horbatsch, R. P. McEachran, and A. D. Stauffer, J. Phys. B **22**, 3763 (1989).
[15] L. Jiao, Y. Zhou, Y. Cheng, and R. M. Yu, Eur. Phys. J. D **66**, 48 (2012).
[16] W. E. Kauppila, C. K. Kwan, T. S. Stein, and S. Zhou, J. Phys. B **27**, L551 (1994).
[17] C. K. Kwan, W. E. Kauppila, R. A. Lukaszew, S. P. Parikh, T. S. Stein, Y. J. Wan, and M. S. Dababneh, Phys. Rev. A **44**, 1620 (1991).

[18] S. Zhou, S. P. Parikh, W. E. Kauppila, C. K. Kwan, D. Lin, A. Surdutovich, and T. S. Stein, Phys. Rev. Lett. **73**, 236 (1994).
[19] E. Surdutovich, J. M. Johnson, W. E. Kauppila, C. K. Kwan, and T. S. Stein, Phys. Rev. A **65**, 032713 (2002).
[20] Z. C. Yan and Y. K. Ho, Phys. Rev. A **77**, 030701(R) (2008).
[21] I. Shimamura, H. Wakimoto, and A. Igarashi, Phys. Rev. A **80**, 032708 (2009).
[22] M. Umair and S. Jonsell, J. Phys. B **47**, 225001 (2014).
[23] M. W. J. Bromley, J. Mitroy, and K. Varga, Phys. Rev. A **75**, 062505 (2007).
[24] P. Fuentealba and O. Reyes, J. Phys. B **26**, 2245 (1993).
[25] J. Mitroy, M. W. J. Bromley, and G. G. Ryzhikh, J. Phys. B **35**, R81 (2002).
[26] NIST Atomic Spectra Database, version 3, http://physics.nist.gov/PhysRefData/ASD/index.html.
[27] M. Kamimura, Phys. Rev. A **38**, 621 (1988).
[28] E. Hiyama, Y. Kino, and M. Kamimura, Prog. Part. Nucl. Phys. **51**, 223 (2003).
[29] J. Hanssen, R. Mccarroll, and P. Valiron, J. Phys. B **12**, 899 (1979).
[30] W. Schweizer and P. Fabbinder, At. Data Nucl. Data Tables **72**, 33 (1999).
[31] W. R. Johnson, D. Kolb, and K.-N. Huang, At. Data Nucl. Data Tables **28**, 333 (1983).
[32] C.-N. Liu and A. F. Starace, Phys. Rev. A **59**, 3643 (1999).
[33] W. P. Reinhardt, Annu. Rev. Phys. Chem. **33**, 223 (1982).
[34] B. R. Junker, Adv. At. Mol. Phys. **18**, 208 (1982).
[35] N. Moiseyev, Phys. Rep. **302**, 212 (1998).
[36] A. Temkin and J. F. Walker, Phys. Rev. **140**, A1520 (1965).
[37] C. M. Surko, G. F. Gribakin, and S. J. Buckman, J. Phys. B **38**, R57 (2005).